Synthesis, Structure, and Reactivity of *rac*-$Me_2Si(indenyl)_2Zr(NMe_2)_2$

Joseph N. Christopher, Gary M. Diamond, and Richard F. Jordan*

Department of Chemistry, University of Iowa, Iowa City, Iowa 52242

Jeffrey L. Petersen

Department of Chemistry, West Virginia University, Morgantown, West Virginia 26506

Received February 13, 1996[⊗]

The amine elimination reaction of $(SBI)H_2$ (**3**, $Me_2Si(1\text{-indenyl})_2$) and $Zr(NMe_2)_4$ (**2**) affords *rac*-$(SBI)Zr(NMe_2)_2$ (**4**) in 65% isolated yield. This reaction proceeds via initial formation of a mono(indenyl) intermediate, (η^5-$C_9H_6SiMe_2C_9H_7$)$Zr(NMe_2)_3$ (**6**). Intermediate **6** reacts reversibly with a second equivalent of **2** to form a binuclear complex, {μ-η^5:η^5-$Me_2Si(1\text{-indenyl})_2$}$\{Zr(NMe_2)_3\}_2$ (**5**), which was prepared independently by the reaction of **3** and 2 equiv of **2**. Complex **6** also undergoes reversible intramolecular amine elimination to form *rac*-**4** and *meso*-**4**. The equilibrium between **6** and **4** + NMe_2H strongly favors **6**. *rac*-**4** is the kinetic product of the intramolecular amine elimination of **6**, the thermodynamic *rac*-**4**/*meso*-**4** ratio is 4/1, and the *rac*-**4**/*meso*-**4** isomerization is catalyzed by NMe_2H. Therefore, the removal of NMe_2H from the reaction mixture is the most important factor in controlling the yield of **4** and the *rac*-**4**/*meso*-**4** ratio. The molecular structures of *rac*-**4** and *meso*-**5** have been determined by X-ray crystallography. *rac*-**4** is cleanly converted to *rac*-$(SBI)ZrCl_2$ (*rac*-**1**, 100% NMR) by reaction with Me_3SiCl and to *rac*-$(SBI)ZrMe_2$ (*rac*-**7**, 92% isolated) by reaction with $AlMe_3$.

Introduction

Chiral group 4 *ansa*-metallocenes, originally developed by Brintzinger,[1] are precursors to highly active catalysts for the stereoselective polymerization of α-olefins and other monomers[2] and are of interest for other applications.[3] The reactivity and stereoselectivity of these catalysts can be modified by varying the metal and the structure of the *ansa*-bis(cyclopentadienyl) ligand. Of the zirconocene catalysts reported to date, SiR_2-bridged bis(indenyl) complexes such as *rac*-$(SBI)ZrCl_2$ (*rac*-**1**, SBI = $Me_2Si(1\text{-indenyl})_2$) and derivatives with substituents at the 2,2′ and 4,4′ positions exhibit the best overall performance in isotactic propylene polymerization.[2e−f,2k]

Chiral *ansa*-metallocenes are normally prepared by chloride displacement reactions of MCl_x compounds and bis(cyclopentadienyl) dianion reagents. However, this method is often inefficient and plagued by low yields and tedious separation and purification steps.[1,3] For example, Herrmann first prepared *rac*-**1** in 14% yield by reaction of $ZrCl_4(THF)_2$ and $(SBI)Li_2$.[4] More recently, Diefenbach has obtained LiCl-free *rac*-**1** in 47% yield.[5]

We recently reported that the amine elimination reaction of $(EBI)H_2$ (1,2-bis(3-indenyl)ethane) and $Zr(NMe_2)_4$ (**2**) provides a highly stereoselective and efficient route to *rac*-$(EBI)Zr(NMe_2)_2$ (EBI = ethylene-1,2-bis(1-indenyl)).[6] This reaction involves initial formation of the mono(indenyl) intermediate (η^5-$C_9H_6CH_2CH_2C_9H_7$)-$Zr(NMe_2)_3$, which undergoes reversible amine elimination reactions to give (μ-η^5:η^5-EBI)$\{Zr(NMe_2)_3\}_2$, *meso*-$(EBI)Zr(NMe_2)_2$, or the thermodynamic product *rac*-$(EBI)Zr(NMe_2)_2$, which is isolated in 68% yield. *rac*-$(EBI)Zr(NMe_2)_2$ can be cleanly converted to the commonly used catalyst precursors *rac*-$(EBI)ZrCl_2$ and *rac*-(EBI)-$ZrMe_2$ by reaction with Me_3SiCl and $AlMe_3$, respectively, and may be activated directly for olefin polymerization.[7] The amine elimination reaction of $(EBI)H_2$ has been extended to other metals (Hf, Y), amides, and *ansa*-bis(cyclopentadienyl) ligands.[6] Here we describe the syn-

[⊗] Abstract published in *Advance ACS Abstracts,* August 15, 1996.

(1) (a) Schnutenhaus, H.; Brintzinger, H. H. *Angew. Chem.* **1979**, *91*, 837; *Angew. Chem., Int. Ed. Engl.* **1979**, *18*, 777. (b) Wild, F. R. W. P.; Zsolnai, L.; Huttner, G.; Brintzinger, H. H. *J. Organomet. Chem.* **1982**, *232*, 233. (c) Wild, F. R. W. P.; Wasiucionek, M.; Huttner, G.; Brintzinger, H. H. *J. Organomet. Chem.* **1985**, *288*, 63.

(2) Leading references: (a) Thayer, A. M. *Chem. Eng. News* **1995**, *73* (37), 15. (b) Brintzinger, H. H.; Fischer, D.; Mülhaupt, R.; Rieger, B.; Waymouth, R. M. *Angew. Chem., Int. Ed. Engl.* **1995**, *34*, 1143. (c) Sinclair, K. B.; Wilson, R. B. *Chem. Ind.* **1994**, 857. (d) Möhring, P. C.; Coville, N. J. *J. Organomet. Chem.* **1994**, *479*, 1. (e) Stehling, U.; Diebold, J.; Kirsten, R.; Roll, W.; Brintzinger, H. H.; Jungling, S.; Mülhaupt, R.; Langhauser, F. *Organometallics* **1994**, *13*, 964. (f) Spaleck, W.; Kuber, F.; Winter, A.; Rohrmann, J.; Bachmann, B.; Antberg, M.; Dolle, V.; Paulus, E. F. *Organometallics* **1994**, *13*, 954. (g) Horton, A. D. *Trends Polym. Sci.* **1994**, *2*, 158. (h) Farina, M. *Trends Polym. Sci.* **1994**, *2*, 80. (i) Bochmann, M. *Nachr. Chem. Tech. Lab.* **1993**, *41*, 1220. (j) Kaminsky, W.; Engehausen, R.; Zoumis, K.; Spaleck, W.; Rohrmann, J. *Makromol. Chem.* **1992**, *193*, 1643. (k) Spaleck, W.; Antberg, M.; Rohrmann, J.; Winter, A.; Bachmann, B.; Kiprof, P.; Behm, J.; Herrmann, W. A. *Angew. Chem., Int. Ed. Engl.* **1992**, *31*, 1347. (l) Ewen, J. A.; Elder, M. J.; Jones, R. L.; Haspeslagh, L.; Atwood, J. L.; Bott, S. G.; Robinson, K. *Makromol. Chem., Macromol. Symp.* **1991**, *48/49*, 253. (m) Spaleck, W.; Antberg, M.; Dolle, V.; Klein, R.; Rohrmann, J.; Winter, A. *New J. Chem.* **1990**, *14*, 499. (n) Kaminsky, W.; Kulper, K.; Brintzinger, H. H.; Wild, F. R. W. P. *Angew. Chem.* **1985**, *97*, 507. (o) Ewen, J. A. *J. Am. Chem. Soc.* **1984**, *106*, 6355.

(3) Halterman, R. L. *Chem. Rev.* **1992**, *92*, 965.

(4) Herrmann, W. A.; Rohrmann, J.; Herdtweck, E.; Spaleck, W.; Winter, A. *Angew. Chem., Int. Ed. Engl.* **1989**, *28*, 1511.

(5) (a) Diefenbach S. P.; Ao, M. S.; Power, J. M.; Strickler, J. R. U.S. patent 5,302,703, 1994. See also: (b) Van Beek, J. A. M. Eur. Pat. Appl. 0 530 908 A1, 1992.

(6) (a) Diamond, G. M.; Rodewald, S.; Jordan, R. F. *Organometallics* **1995**, *14*, 5. (b) Diamond, G. M.; Jordan, R. F.; Petersen, J. L., *J. Am. Chem. Soc.*, in press. (c) Diamond, G. M.; Jordan, R. F.; Petersen, J. L. *Organometallics* **1996**, *15*, 4030. (d) Diamond, G. M.; Jordan, R. F., Petersen, J. L. *Organometallics* **1996**, *15*, 4045. (e) Ross, K. J.; Swenson, D. C.; Jordan, R. F.; Rogers, R. D. Manuscript in preparation.

(7) Kim, I.; Jordan, R. F. *Macromolecules* **1996**, *29*, 489.

S0276-7333(96)00104-5 CCC: $12.00

thesis of *rac*-(SBI)$Zr(NMe_2)_2$ and several derivatives by amine elimination chemistry.

Results and Discussion

Synthesis and Properties of (SBI)H_2 (3). As previously reported by several authors, the reaction of Me_2SiCl_2 and 2 equiv of lithium indenide affords $Me_2Si(1\text{-indenyl})_2$ (**3**, (SBI)H_2) as a mixture of *rac* and *meso* 1-substituted isomers (eq 1), from which *rac*-**3** is isolated

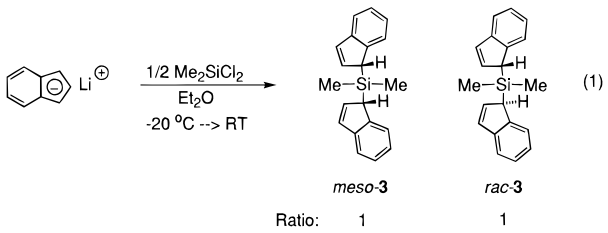

(1)

as a white solid by selective crystallization from Et_2O at −80 °C.[8−10] A detailed study by McGlinchey showed that *rac*-**3** and *meso*-**3** undergo thermal interconversion by successive 1,5-sigmatropic silyl shifts and an isoindene intermediate and that this is the only operative isomerization mechanism below 200 °C.[10,11] We found that the reaction of Me_2SiCl_2 and 2 equiv of lithium indenide on a 35 g scale produces a 1/1 mixture of *rac*-**3** and *meso*-**3** in 95% yield as a pale yellow solid (>95% pure by ^{1}H NMR). This material was used directly in subsequent reactions.

Synthesis of *rac*-(SBI)$Zr(NMe_2)_2$ (*rac*-4). The reaction of $Zr(NMe_2)_4$ (**2**) and **3** in refluxing hexanes under N_2 for 8 h, in a reaction flask equipped with a water-cooled fractional distillation column packed with glass helices, affords (SBI)$Zr(NMe_2)_2$ (**4**) in 75% NMR yield in a *rac*/*meso* ratio of 14/1. Crystallization from hexanes affords pure *rac*-**4** as red crystals in 65% isolated yield (eq 2). *rac*-**4** was characterized by ^{1}H and

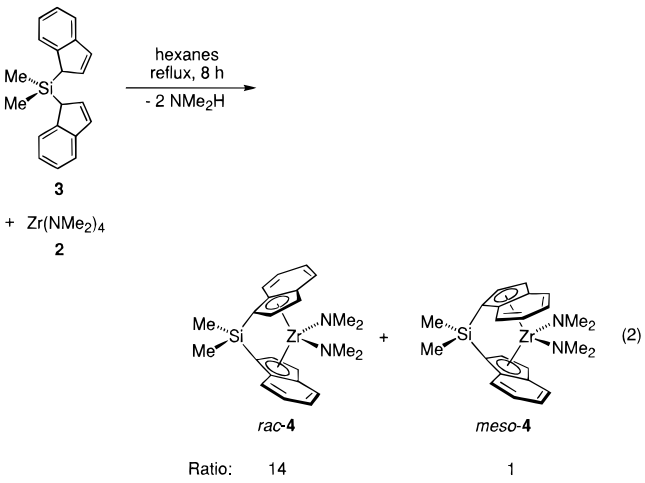

(2)

^{13}C NMR, elemental analysis, and an X-ray crystal structure determination which confirmed the monomeric structure and stereochemistry (vide infra). The minor *meso* isomer was identified by ^{1}H NMR spectroscopy. The ^{1}H NMR spectrum of the C_2-symmetric *rac*-**4** contains one $SiMe_2$ and one NMe_2 resonance; in contrast, the spectrum of the C_s-symmetric *meso* isomer contains two $SiMe_2$ and two NMe_2 resonances.

Reaction Mechanism and Stereocontrol. The mechanism and the origin of the stereoselectivity observed in the reaction depicted in eq 2 were investigated by NMR studies and model reactions. These studies are consistent with the mechanism shown in Scheme 1, which is analogous to that established for the amine elimination synthesis of *rac*-(EBI)$Zr(NMe_2)_2$.[6] Key observations are summarized below.

(i) The reaction of **2** and **3** in C_6D_6 in a closed system (from which the NMe_2H cannot escape) proceeds rapidly (10 min) at 25 °C and yields a 6/1 mixture of the mono(indenyl) Zr complex (η^5-$C_9H_6SiMe_2C_9H_7$)$Zr(NMe_2)_3$ (**6a**−**c**)[12] and a binuclear complex {μ-η^5:η^5-$Me_2Si(indenyl)_2$}-{$Zr(NMe_2)_3$}$_2$ (**5**, 1/1 *rac*/*meso* ratio), along with NMe_2H and unreacted **3** (Scheme 1). After 24 h at 23 °C, the **6**/**5** product ratio decreases to 1.8/1, which is close to the statistical ratio expected (2/1) if the indene groups of **3** react independently.[13] Addition of **3** (2 equiv based on Zr) results in conversion of **5** to **6**; *i.e.*, the $Zr(NMe_2)_4$ which is released by reaction of **5** with NMe_2H is trapped by **3** yielding **6**. After 43 h the **6**/**5** ratio = 6.5/1.[13b] These observations indicate that the initial amine elimination reaction of **2** and **3** to form mono(indenyl) species **6** is rapid at 23 °C and that the amine elimination reaction of **6** with a second equivalent of **2** is reversible.

Complex **6** was identified by ^{1}H NMR spectroscopy. This species exists as three isomers (Scheme 1) which differ in the site of attachment of the $SiMe_2$ bridge to the pendant indene group; in the major isomers (**6a,b**), the $SiMe_2$ bridge is located at the 1-position, while, in the minor isomer (**6c**), the $SiMe_2$ bridge is located at the 3-position. Isomers **6a,b** can be identified by the relative intensities of the two $SiMe_2$ resonances and the allylic (bridgehead) hydrogen resonance (3/3/1) but cannot be distinguished from each other. Isomer **6c** is distinguished from **6a,b** by the 3/3/2 ratio of the $SiMe_2$ and allylic hydrogen resonances.

Complex **5** was prepared in 90% NMR yield in a *rac*/*meso* ratio of 1/2, by the reaction of **3** with 2 equiv of **2** (toluene, 23 °C, 21 h). Crystallization from hexanes affords pure *meso*-**5** as orange crystals in 34% yield. *meso*-**5** was characterized by ^{1}H and ^{13}C NMR, elemental analysis, and an X-ray crystal structure determination which confirmed the binuclear structure (vide

(8) (a) Marechal, E.; Tortal, J. P. *C. R. Acad. Sci. Paris* **1968**, *267*, 467. (b) Sommer, L. H.; Marans, N. S. *J. Am. Chem. Soc.* **1951**, *73*, 5135.

(9) Others have reported that the crude mixture also contains $Me_2Si(3\text{-indenyl})_2$, but the reported NMR data are inconsistent with this structure. The observation of two doublets for the $SiMe_2$ groups is inconsistent with the C_2 symmetry of this species. See: Chen, Y. X.; Rausch, M. D.; Chien, J. C. W. *Organometallics* **1993**, *12*, 4607.

(10) (a) Rigby, S. S.; Girard, L.; Bain, A. D.; McGlinchey, M. J. *Organometallics* **1995**, *14*, 3798 and references therein. (b) Rigby, S. S.; Gupta, H. K.; Werstiuk, N. H.; Bain, A. D.; McGlinchey, M. J. *Polyhedron* **1995**, *14*, 2787.

(11) In a C_6D_6 solution (sealed tube), *rac*-**3** isomerizes to a 1/1 mixture of the *rac* and *meso* isomers after several hours at 50 °C. This mixture is stable at 100 °C (>24 h), but after 24 h at 150 °C a mixture of several unidentified compounds is produced.

(12) For $CpM(NR_2)_3$ compounds see: (a) Martín, A.; Mena, M.; Yélamos, C.; Serrano, R.; Raithby, P. R. *J. Organomet. Chem.* **1994**, *467*, 79. (b) Galakhov, M.; Martín, A.; Mena, M.; Yélamos, C. *J. Organomet. Chem.* **1995**, *496*, 217. (c) Bai, Y.; Roesky, H. W.; Noltemeyer, M.; Witt, M. *Chem. Ber.* **1992**, *125*, 825. (d) Bürger, H.; Dämmgen, U. *J. Organomet. Chem.* **1975**, *101*, 295. (e) Bürger, H.; Dämmgen, U. *J. Organomet. Chem.* **1975**, *101*, 307. (f) Chandra, G.; Lappert, M. F. *J. Chem. Soc. A* **1968**, 1940.

(13) (a) The equilibrium constant K_{eq} for **6** = **5** + **3** (which is catalyzed by NMe_2H) is 0.31(3) at 23 °C in C_6D_6. (b) The final observed ratio **3**/**6**/**5** = 20/6.5/1 is in agreement with that predicted by the K_{eq} value noted above (21/6.4/1).

Scheme 1

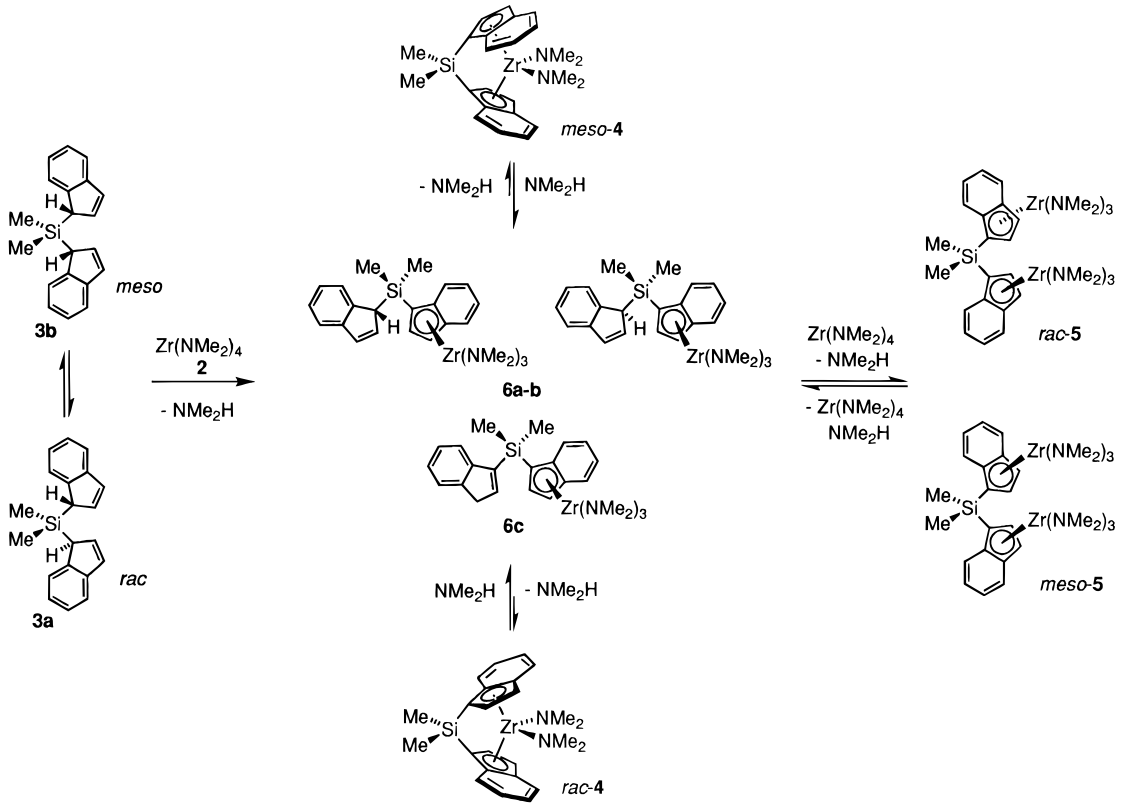

infra), and *rac*-**5** was characterized by ^{1}H NMR spectroscopy. The ^{1}H NMR spectrum of the C_s-symmetric *meso*-**5** contains two $SiMe_2$ resonances, while that of the C_2-symmetric *rac* isomer contains one $SiMe_2$ resonance.

(ii) As noted above, **2** and **3** react rapidly at 23 °C in a closed system to yield **5**, **6**, NMe_2H, and unreacted **3**. Complex **4** is not formed under these conditions. The lack of formation of **4** could be due to a slow rate of intramolecular amine elimination from **6** or to an unfavorable equilibrium between **6** and **4** + NMe_2H. To investigate these possibilities, the effect of removing NMe_2H from the mixture was studied.

A Teflon-valved NMR tube was charged with a solution of **2** and **3** in C_6D_6, sealed, and maintained at 23 °C. Periodically, the tube was opened, the volatiles (NMe_2H and C_6D_6) were removed under vacuum and replaced with fresh C_6D_6, and the ^{1}H NMR spectrum was recorded. The concentrations of Zr species were determined by NMR integration versus an internal standard. The results of this experiment are illustrated graphically in Figure 1.

As expected from above, **2** and **3** reacted rapidly to yield a mixture of intermediates **5** and **6** and NMe_2H; no **4** was formed even after 18 h. At this point, removal of the volatiles and addition of fresh C_6D_6 resulted in rapid (<10 min) formation of 10% **4** (4/1 *rac*/*meso* ratio) at the expense of **5** and **6** but no further change for 16 h. Repeating this procedure resulted in successive rapid incremental increases in the concentration of **4** and corresponding decreases in the concentration of **5** + **6**, until new plateaus were reached. After 47 h, NMe_2H (1.3 equiv based on Zr) was added, and rapid (<10 min) conversion of **4** back to **5** and **6** was observed. These observations establish that the intramolecular amine elimination reaction of **6** to **4** is rapid at 23 °C but that the equilibrium between **6** and **4** + NMe_2H strongly favors **6**.

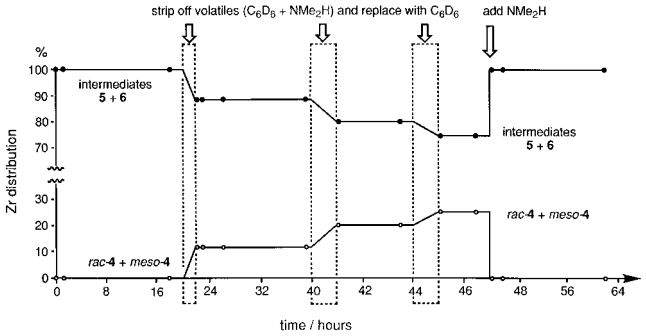

Figure 1. Time dependence of the distribution of Zr species (% total Zr) in the reaction of **2** and **3** (Scheme 1, C_6D_6, 23 °C). The closed circles represent the fraction **5** + **6**, and the open circles represent the fraction *rac*-**4** + *meso*-**4**. At the time points indicated by arrows, the NMR tube was opened and the volatiles (C_6D_6 and NMe_2H) were removed under vacuum and replaced with fresh C_6D_6. After 47 h, NMe_2H (1.3 equiv) was added. The mass balance of the Zr species was >95% over the course of the experiment as determined by NMR integration versus an internal standard. Note that the time scale is not linear; the region between 40 and 48 h has been expanded for clarity.

(iii) In the experiment outlined in Figure 1, a 4/1 *rac*-**4**/*meso*-**4** ratio was observed at each equilibrium point. However, when the reaction of **2** and **3** (*m*-xylene, 25 °C) with an N_2 purge was monitored by ^{1}H NMR, it was observed that the *rac*/*meso* ratio of product **4** was initially high (13/1 after 12 h; 50% conversion to **4**) but gradually decreased to 4/1 after 24 h (75% conversion to **4**). These observations indicate that *rac*-**4** is the kinetic product of the intramolecular amine elimination

Table 1. Summary of Crystallographic Data

compd	*rac*-(SBI)$Zr(NMe_2)_2$ (*rac*-**4**)	*meso*-{μ-η^5:η^5(SBI)}{$Zr(NMe_2)_3$}$_2$ (*meso*-**5**)
empirical formula	$C_{24}H_{30}N_2SiZr$	$C_{32}H_{54}N_6SiZr_2$
fw	465.81	733.34
temp	295 (2) K	295 (2) K
wavelength	0.710 73 Å	0.710 73 Å
cryst system	monoclinic	monoclinic
space group	*C*2/*c*	*C*2/*c*
unit cell dimens	a = 17.423(1) Å, α = 90°; b = 12.412(1) Å, β = 114.55(1)°; c = 11.253(1) Å, γ = 90°	a = 35.501(2) Å, α = 90°; b = 9.517(1) Å, β = 105.51(1)°; c = 22.906(2) Å, γ = 90°
V	2213.6(3) Å^3	7457.3(11) Å^3
Z	4	8
D(calcd)	1.398 g/cm^3	1.306 g/cm^3
abs coeff	5.63 cm^{-1}	6.19 cm^{-1}
F(000)	968	3056
cryst size	0.28 × 0.32 × 0.50 mm	0.32 × 0.20 × 0.72 mm
θ range for data collcn	2.08−27.50°	1.91−22.50°
index ranges	$-22 \le h \le 22$, $-16 \le k \le 16$, $-14 \le l \le 14$	$0 \le h \le 36$, $0 \le k \le 10$, $-24 \le l \le 23$
reflcns collcd	5041	4860
indepdt reflcns	2535 (R_{int} = 0.0124)	4772 (R_{int} = 0.0338)
refinement method	full-matrix least squares on F^2, non-H anisotropic; H isotropic, fixed	full-matrix least squares on F^2, non-H anisotropic; H isotropic, fixed
data/restraints/params	2463/0/132	4254/0/384
goodness-of-fit on F^2	1.058	1.024
final R indices [$I > 2\sigma(I)$]	$R1$ = 0.0228, w$R2$ = 0.0608	$R1$ = 0.0468, w$R2$ = 0.0961
R indices (all data)	$R1$ = 0.0270, w$R2$ = 0.0631	$R1$ = 0.0877, w$R2$ = 0.1146
largest diff peak and hole	0.322 and −0.167 e Å^{-3}	1.058 and −0.315 e Å^{-3}

of **6** and that the 4/1 *rac*-**4**/*meso*-**4** ratio is the thermodynamic product ratio.

(iv) Observations i−iii indicate that the key to the synthesis of *rac*-**4** by the amine elimination reaction of **2** and **3** is to remove NMe_2H rapidly from the system as it is formed.

Practical Considerations. The reaction conditions described above for eq 2 (refluxing hexanes, fractional distillation column) were found to give reasonable and reproducible results. The evolved amine can also be removed by vigorous N_2 purging of the reaction mixture. However, it was found that on the laboratory scale this approach requires longer reaction times and suffers from solvent loss problems, and the conditions are difficult to control and reproduce. Increasing the reaction temperature to > ca. 90 °C results in decreased yields due to thermal decomposition.[14]

Structure and Bonding in *rac*-(SBI)$Zr(NMe_2)_2$. The molecular structure of *rac*-(SBI)$Zr(NMe_2)_2$ (*rac*-**4**) was determined by X-ray diffraction (Figure 2, Tables 1 and 2). *rac*-**4** adopts a monomeric, bent metallocene structure with crystallographically imposed C_2 symmetry and is structurally very similar to *rac*-(EBI)Zr-$(NMe_2)_2$.[6b] The centroid−Zr−centroid angle (122.8°), N−Zr−N angle (97.0°), dihedral angle between the C_5 ring planes (64.1°), Zr−centroid bond length (2.322 Å), and average Zr−C bond length (2.619 Å) are nearly identical to the corresponding values for *rac*-(EBI)Zr-$(NMe_2)_2$ (centroid−Zr−centroid, 122.2°; N−Zr−N, 99.4°; angle between C_5 planes, 62.0°; Zr−centroid, 2.307 and 2.319 Å; average Zr−C, 2.601 and 2.609 Å).[6b] Additionally, the angle between the metal−centroid vector and the C_5 ring plane (88.5°) and the trend in Zr−C bond lengths (Zr−C(3), Zr−C(4) < Zr−C(2), Zr−C(5) < Zr−C(1); see Figure 2 for numbering scheme) are the same for the two compounds. The most significant difference between these structures is that the distances between Zr and the carbons at the front of the metallocene wedge (i.e. Zr−C(1) and Zr−C(2), Figure 2) are ca. 0.04 Å longer for *rac*-**4** than *rac*-(EBI)$Zr(NMe_2)_2$.

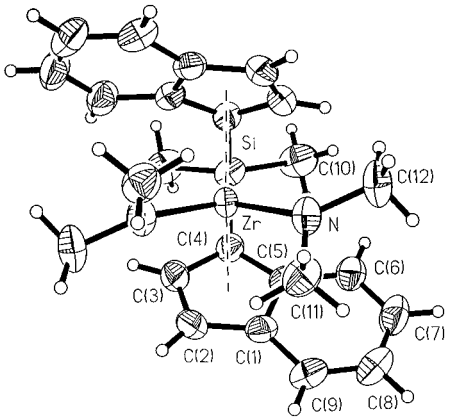

Figure 2. Molecular structure of *rac*-(SBI)$Zr(NMe_2)_2$ (*rac*-**4**).

The metrical parameters for the amide groups of *rac*-**4** are consistent with partial N−Zr π-donation.[15] The amides are flat (sum of angles around N = 359.6°), and the Zr−N distance (2.07 Å) is in the range observed for other unsaturated Zr(IV) amide complexes (2.00−2.17 Å).[16] The dihedral angle between the N−Zr−N and

(14) (a) The reaction of **2** and **3** in *m*-xylene at 60 °C with an N_2 purge afforded **4** in 85% NMR yield in a 10/1 *rac*/*meso* ratio after 46 h. (b) The reaction of **2** and **3** in *m*-xylene without an N_2 purge under more forcing conditions (140 °C, 11 h) afforded **4** in 40% NMR yield (*rac*/*meso* ratio = 7/1) and *rac*-**4** in 31% isolated yield; however, control experiments established that 50−60% loss of zirconium due to thermal decomposition occurs under these conditions.

(15) (a) Lappert, M. F.; Power, P. P.; Sanger, A. R.; Srivastava, R. C. *Metal and Metalloid Amides*; Ellis Horwood: Chichester, West Sussex, U.K., 1980; pp 500−502. (b) Andersen, R. A.; Beach, D. B.; Jolly, W. L. *Inorg. Chem.* **1985**, *24*, 2741. (c) Bradley, D. C.; Chisholm, M. H. *Acc. Chem. Res.* **1976**, *9*, 273.

(16) Representative Zr(IV) amide complexes and average Zr−N distances: (a) $Zr(NMe_2)_4$, 2.07 Å (electron diffraction). Hagen, K.; Holwill, C. J.; Rice, D. A.; Runnacles, J. D. *Inorg. Chem.* **1988**, *27*, 2032. (b) $(Me_2N)_3Zr(\mu\text{-}NMe_2)_2Zr(NMe_2)_3$, terminal Zr−N 2.04−2.11 Å. Chisholm, M. H.; Hammond, C. E.; Huffman, J. C. *Polyhedron* **1988**, *7*, 2515. (c) $(Me_2N)_2Zr(\mu\text{-}N^tBu)_2Zr(NMe_2)_2$, 2.06 Å. Nugent, W. A.; Harlow, R. L. *Inorg. Chem.* **1979**, *18*, 2030. (d) $Cp_2Zr(NC_4H_4)_2$, 2.17 Å. Bynum, R. V.; Hunter, W. E.; Rogers, R. D.; Atwood, J. L. *Inorg. Chem.* **1980**, *19*, 2368. (e) $Cp^*Zr(NPr^i_2)Cl_2$, 2.00 Å. Pupi, R. M.; Coalter, J. N.; Petersen, J. L. *J. Organomet. Chem.* **1995**, *497*, 17. (f) (η^5-$C_2B_9H_{11}$)-$Zr(NEt_2)_2(NHEt_2)$, Zr−NEt_2 = 2.04 Å, Zr−$NHEt_2$ = 2.36 Å. Bowen, D. E.; Jordan, R. F.; Rogers, R. D. *Organometallics* **1995**, *14*, 3630. (g) $(Me_4taen)Zr(NMe_2)_2$, 2.11 Å. Black, D. G.; Swenson, D. C.; Jordan, R. F.; Rogers, R. D. *Organometallics* **1995**, *14*, 3539.

Table 2. Selected Bond Lengths (Å) and Angles (deg) for *rac*(SBI)Zr(NMe$_2$)$_2$ (*rac*-4)[a,b]

Zr−N	2.0718(14)	Zr−C(1)	2.720(2)
Zr−C(2)	2.624(2)	Zr−C(3)	2.539(2)
Zr−C(4)	2.562(2)	Zr−C(5)	2.648(2)
Si−C(10)	1.855(2)	Si−C(4)	1.862(2)
N−C(12)	1.450(2)	N−C(11)	1.462(2)
C(1)−C(2)	1.414(3)	C(1)−C(9)	1.419(3)
C(1)−C(5)	1.436(2)	C(2)−C(3)	1.410(3)
C(3)−C(4)	1.425(2)	C(4)−C(5)	1.439(2)
C(5)−C(6)	1.423(2)	C(6)−C(7)	1.362(3)
C(7)−C(8)	1.405(3)	C(8)−C(9)	1.353(3)
N−Zr−N′	96.98(8)	Cp(c)−Zr−Cp′(c)	122.8
Cp(c)−Zr−N	108.5	C(4)−Si−C(4)′	95.72(10)
C(4)−Si−C(10)	113.56(9)	C(10)−Si−C(10)′	110.3(2)
C(4)′−Si−C(10)′	111.52(10)	C(11)−N−Zr	118.49(11)
C(12)−N−Zr	131.57(13)	C(12)−N−C(11)	109.5(2)
C(2)−C(1)−C(9)	132.5(2)	C(2)−C(1)−C(5)	107.8(2)
C(9)−C(1)−C(5)	119.7(2)	C(3)−C(2)−C(1)	107.5(2)
C(2)−C(3)−C(4)	110.6(2)	C(3)−C(4)−C(5)	105.3(2)
C(3)−C(4)−Si	124.05(13)	C(5)−C(4)−Si	127.45(13)
C(6)−C(5)−C(1)	118.8(2)	C(6)−C(5)−C(4)	132.5(2)
C(1)−C(5)−C(4)	108.7(2)	C(7)−C(6)−C(5)	119.1(2)
C(6)−C(7)−C(8)	121.6(2)	C(9)−C(8)−C(7)	121.4(2)
C(8)−C(9)−C(1)	119.2(2)		

[a] Symmetry transformations used to generate equivalent (′) atoms: $-x, y, -z + {}^1/_2$. [b] Cp(c) denotes the centroid of the five-membered ring of the indenyl group.

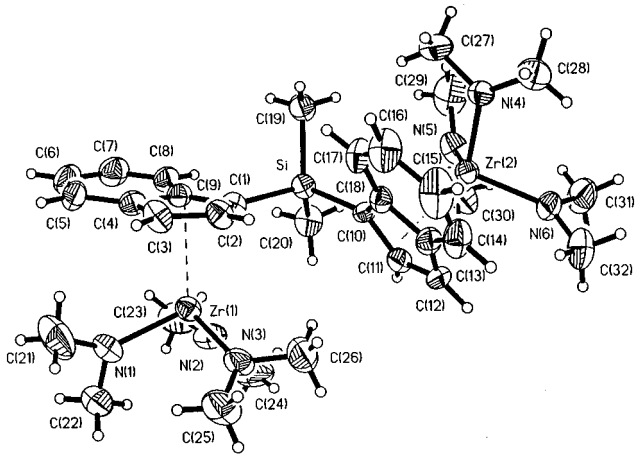

Figure 3. Molecular structure of *meso*-{μ-η^5:η^5-(SBI)}{Zr(NMe$_2$)$_3$}$_2$ (*meso*-**5**).

amide C−N−C planes is 38.7°. Steric crowding between the SBI ligand framework and the NMe$_2$ ligands prevents the amides from adopting a more perpendicular orientation which would maximize π-bonding.[17] Additionally, the Zr−N(1)−C(12) and Zr−N(2)−C(12′) angles are widened from the sp^2 value (120°) to 131.6°, and the C−N−C angles are narrowed to 109.5° due to SBI−amide steric interactions. The corresponding metrical parameters for *rac*-(EBI)Zr(NMe$_2$)$_2$ are all very similar: Zr−N distances, 2.061, 2.053 Å; N−Zr−N/C−N−C dihedral angles 34.6, 35.4°; Zr−N−C angles 131.0 and 111.1° (N(1)), 130.6 and 108.8° (N(2)).[6b]

Structure of {μ-η^5:η^5-Me$_2$Si(indenyl)$_2$}{Zr(NMe$_2$)$_3$}$_2$. The molecular structure of *meso*-**5** was determined by single-crystal X-ray diffraction (Figure 3, Tables 1 and 3). *meso*-**5** adopts a binuclear structure in which the SBI ligand bridges two Zr(NMe$_2$)$_3$ units. The two indenyl groups are rotated by approximately 45° from coplanarity. The Zr centroid distances (2.324, 2.312 Å) and Zr−C distances (2.546−2.696 Å) are

Table 3. Selected Bond Lengths (Å) and Angles (deg) for *meso*-{μ-η^5:η^5(SBI)}{Zr(NMe$_2$)$_3$}$_2$ (*meso*-5)

Zr(1)−N(1)	2.052(6)	Zr(2)−N(4)	2.027(5)
Zr(1)−N(2)	2.033(6)	Zr(2)−N(5)	2.037(5)
Zr(1)−N(3)	2.028(5)	Zr(2)−N(6)	2.037(5)
Zr(1)−Cp(c)(1)[a]	2.324	Zr(2)−Cp(c)(2)[a]	2.312
Si−C(1)	1.870(6)	Si−C(10)	1.856(6)
Si−C(19)	1.874(6)	Si−C(20)	1.861(6)
N(1)−Zr(1)−N(2)	104.8(2)	N(4)−Zr(2)−N(5)	104.2(2)
N(1)−Zr(1)−N(3)	98.3(2)	N(4)−Zr(2)−N(6)	101.4(2)
N(2)−Zr(1)−N(3)	102.7(3)	N(5)−Zr(2)−N(6)	101.8(2)
C(21)−N(1)−C(22)	108.4(6)	C(27)−N(4)−C(28)	109.3(6)
C(21)−N(1)−Zr(1)	134.7(5)	C(27)−N(4)−Zr(2)	122.5(4)
C(22)−N(1)−Zr(1)	116.6(5)	C(28)−N(4)−Zr(2)	127.8(4)
C(23)−N(2)−C(24)	109.8(7)	C(29)−N(5)−C(30)	111.2(6)
C(23)−N(2)−Zr(1)	119.5(5)	C(29)−N(5)−Zr(2)	129.9(6)
C(24)−N(2)−Zr(1)	130.7(6)	C(30)−N(5)−Zr(2)	118.4(5)
C(25)−N(3)−C(26)	109.9(6)	C(31)−N(6)−C(32)	108.2(5)
C(25)−N(3)−Zr(1)	129.4(5)	C(31)−N(6)−Zr(2)	120.9(5)
C(26)−N(3)−Zr(1)	120.5(5)	C(32)−N(6)−Zr(2)	130.5(5)

[a] Cp(c)(1) and Cp(c)(2) denote the centroids of the five-membered rings of the indenyl groups.

essentially identical to those of *rac*-**4**. The Zr centers adopt three-legged piano-stool geometries in which the N−Zr−N angles range from 98.3 to 104.8° and the centroid−Zr−N angles range from 110.8 to 120.4°. The amide groups of *meso*-**5** are flat (sum of angles around N 359.5−360.0°; Zr−N bond lengths range from 2.027 Å to 2.052 Å, consistent with the expected N−Zr π-donation).[15,16]

Comparison of (SBI)Zr(NMe$_2$)$_2$ and (EBI)Zr(NMe$_2$)$_2$ Syntheses. The reactions of (SBI)H$_2$ and (EBI)H$_2$ with Zr(NMe$_2$)$_4$ yield (SBI)Zr(NMe$_2$)$_2$ and (EBI)Zr(NMe$_2$)$_2$ by analogous mechanisms (Scheme 1). However, the reaction dynamics and stereoselectivity features are quite different for the two systems.

The first amine elimination to form the mono(indenyl) intermediate (**6**), and the intramolecular amine elimination of **6** to form **4**, are both faster for the SBI system than the EBI system. It has been shown that 9-Me$_3$Si-fluorene is more acidic than 9-Me-fluorene (pK_a in Me$_2$SO: 9-Me$_3$Si-fluorene, 21.7; 9-Me-fluorene, 22.3).[18] The pK_as for the indenyl analogs are not available but are expected to follow the same trend, which may explain the faster amine eliminations observed in the SBI system versus the EBI system. The shorter Me$_2$Si versus CH$_2$CH$_2$ bridge may also favor cyclization to the *ansa*-metallocene for SBI versus EBI.

The reverse reaction of the *ansa*-metallocenes **4** with NMe$_2$H to form the mono(indenyl) intermediate **6** is also faster for SBI than EBI. This reaction likely proceeds via initial coordination of NMe$_2$H and subsequent proton transfer to an indenyl C$_5$ ring. As the molecular structures of *rac*-**4** and *rac*-(EBI)Zr(NMe$_2$)$_2$ are essentially identical except for the bridging groups as discussed in detail above, this reactivity difference is probably electronic in origin. Recent experimental and theoretical studies suggest that the Me$_2$SiCp$_2$ ligand is electron withdrawing relative to the unbridged Cp$_2$ ligand system in Zr(IV) compounds.[19] Thus zirconocenes with Me$_2$Si-bridged ligands may be stronger Lewis acids and have a higher tendency to coordinate NMe$_2$H and undergo subsequent Zr−indenyl aminolysis than −CH$_2$−CH$_2$− bridged analogues. Also, if the departing indene

(17) Lauher, J. W.; Hoffmann, R. *J. Am. Chem. Soc.* **1976**, *98*, 1729.

(18) (a) Bordwell, F. G. *Acc. Chem. Res.* **1988**, *21*, 456. (b) Streitwieser, A.; Xie, L.; Wang, P.; Bachrach, S. M. *J. Org. Chem.* **1993**, *58*, 1778.

Scheme 2

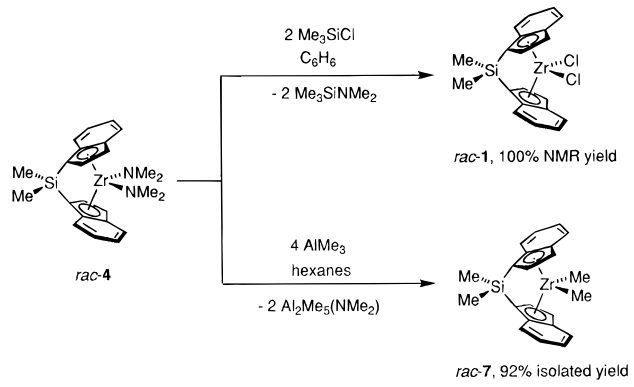

group develops significant carbanionic (Ind^-) character in the transition state for proton transfer, then factors that increase IndH acidity (i.e. silyl versus alkyl substituents) would stabilize the transition state and accelerate the aminolysis reaction. Indeed, in one limiting mechanistic possibility, the amine may displace the Ind^- group completely prior to proton transfer. It should be noted that the relative rates of conversion of the mono(indenyl) intermediate to metallocene product (SBI > EBI), and the relative stabilities of the metallocene product versus the mono(indenyl) intermediate + NMe_2H (SBI < EBI) in the SBI and EBI systems together ensure that $(SBI)Zr(NMe_2)_2$ will react faster with NMe_2H than will $(EBI)Zr(NMe_2)_2$.

For $(EBI)Zr(NMe_2)_2$ the *rac* isomer is the thermodynamically favored product, and the kinetic *rac*/*meso* product ratio is 1/1. In contrast, for $(SBI)Zr(NMe_2)_2$ the thermodynamic *rac*/*meso* ratio is 4/1, and the *rac* isomer is the kinetic product.

Reactivity of *rac*-$(SBI)Zr(NMe_2)_2$. *rac*-**4** is cleanly and stereospecifically converted to *rac*-$(SBI)ZrCl_2$ (*rac*-**1**) and *rac*-$(SBI)ZrMe_2$ (*rac*-**7**) using procedures developed for *rac*-$(EBI)Zr(NMe_2)_2$ (Scheme 2). The reaction of *rac*-**4** with excess[20] Me_3SiCl (hexanes, 23 °C, 24 h) affords *rac*-**1** in high yield (>95% NMR from *rac*-**4**, 52% isolated from $Zr(NMe_2)_4$) with no sign of isomerization. The reaction of *rac*-**4** with excess (>4 equiv) $AlMe_3$ (toluene, 23 °C, 2 h) yields *rac*-**7** (92% isolated). *rac*-**1** and *rac*-**7** are standard precursors for olefin polymerization catalysts.[2] Alternatively, as described in detail elsewhere, *rac*-**4** may be activated for olefin polymerization by in-situ alkylation ($AlMe_3$) followed by reaction with MAO or cationic activators (Ph_3C^+, HNR_3^+).[7]

Conclusion

Amine elimination provides an efficient entry to *rac*-$(SBI)ZrX_2$ (X = NMe_2, Cl, Me) complexes. *rac*-$(SBI)Zr(NMe_2)_2$ (*rac*-**4**) can be prepared in high yield and with high stereoselectivity by the amine elimination reaction of $Zr(NMe_2)_4$ (**2**) and $Me_2Si(1\text{-indenyl})_2$ (**3**, 1/1 *rac*/*meso* mixture). The removal of NMe_2H from the reaction mixture is the most important factor in controlling the yield of **4** and the *rac*-**4**/*meso*-**4** ratio. When the amine is not removed, the mono(indenyl) complex **6** and the binuclear complex **5** are the major products. The kinetic metallocene product is *rac*-**4**, and the thermodynamic *rac*-**4**/*meso*-**4** ratio is 4/1. The intermolecular and intramolecular amine elimination reactions of **2**, **3**, and **6** are faster than the corresponding reactions in the (EBI)-H_2/$(EBI)Zr(NMe_2)_2$ system, due to the higher acidity of $(SBI)H_2$ and the pendant indene in **6** versus $(EBI)H_2$ and the pendant indene in $(\eta^5\text{-}C_9H_6CH_2CH_2C_9H_7)Zr(NMe_2)_3$. The reverse reactions of *rac*-**4** and *meso*-**4** with NMe_2H leading to **6** are also faster than for $(EBI)Zr(NMe_2)_2$. One possible explanation is that *rac*-**4** is a stronger Lewis acid than *rac*-$(EBI)Zr(NMe_2)_2$. *rac*-**4** is cleanly converted to *rac*-**1** by amide−halide exchange with Me_3SiCl and to *rac*-**7** via alkylation of *rac*-**4** with $AlMe_3$ and can be activated for olefin polymerization. The extension of this methodology to the synthesis of more highly substituted $SiMe_2$-bridged metallocenes is under investigation.

Experimental Section

General Procedures. All manipulations were performed using glovebox or Schlenk techniques under a purified N_2 atmosphere. Solvents were distilled from appropriate drying/deoxygenating agents and stored under N_2 prior to use: toluene, hexane, Et_2O, and benzene-d_6 (Na/benzophenone); *m*-xylene (molecular sieves). Me_2SiCl_2 was stirred over quinoline overnight, distilled, and stored under N_2 at 5 °C. $Zr(NMe_2)_4$ was prepared using procedures described in previous papers in this series.[6] NMR spectra were recorded on a Bruker AMX-360 instrument in flame-sealed or Teflon-valved tubes at 25 °C, unless otherwise indicated. ^1H and ^{13}C chemical shifts are reported versus Me_4Si and were determined by reference to the residual solvent peaks. Elemental analyses were performed by E&R Microanalytical Laboratory, Inc.

Lithium Indenide. A flask was charged with indene (90%, 50 mL, 0.38 mol) and hexane (500 mL). N_2 gas was bubbled through the solution for 30 min. BuLi (2.5 M in hexanes, 150 mL, 0.38 mol) was added over 30 min yielding a cream-colored slurry. The slurry was stirred at 23 °C for 18 h and filtered. The pale cream-colored solid was washed with hexane (175 mL) and dried under vacuum (41 g, 88%).

$Me_2Si(1\text{-indenyl})_2$ (3). A modified literature procedure was employed.[8] A solution of Me_2SiCl_2 (19.5 g, 150 mmol) in Et_2O (100 mL) was added dropwise to a solution of lithium indenide (36.0 g, 295 mmol) in Et_2O (150 mL) at −78 °C over 2 h. The tan slurry was allowed to warm to 23 °C, stirred for 18 h, and quenched with ice water (200 mL). The two phases were separated, and the aqueous layer was extracted with Et_2O (3 × 100 mL). The organic phase and the ether wash were combined, washed with water (3 × 100 mL), and dried over Na_2SO_4. The solvent was removed under reduced pressure yielding a yellow solid (40.5 g, 95.3%). The ^1H NMR spectrum established that this product was a 1/1 mixture of *rac*-**3** and *meso*-**3** (>95% purity).

***rac*-$(SBI)Zr(NMe_2)_2$ (*rac*-4).** A three-neck round bottom flask was charged with $(SBI)H_2$ (712 mg, 2.46 mmol), $Zr(NMe_2)_4$ (660 mg, 2.46 mmol), and hexanes (50 mL). The flask was fitted with a H_2O-cooled fractional distillation column (25 cm × 2 cm) packed with 3 mm glass helices. The two other necks were fitted with a stopcock and a stopper. The reaction mixture was refluxed for 8 h while a N_2 flow was maintained over the top of the column. An aliquot was removed and analyzed by ^1H NMR, which revealed the presence of *rac*-**4** (70%) *meso*-**4** (5%), **6a**−**c** (13%), and *rac*- and *meso*-**5** (12%). The solvent was removed under reduced pressure affording an orange solid. The solid was extracted with hexanes (120

(19) (a) Alameddin, N. G.; Ryan, M. F.; Eyler, J. R.; Siedle, A. R.; Richardson, D. E. *Organometallics* **1995**, *14*, 5005. (b) Bajgur, C. S.; Tikkanen, W. R.; Petersen, J. L. *Inorg. Chem.* **1985**, *24*, 2539. (c) Woo, T. K.; Fan, L.; Ziegler, T. *Organometallics* **1994**, *13*, 2252. (d) Siedle, A. R.; Newmark, R. A.; Lamanna, W. M.; Schroepfer, J. N. *Polyhedron* **1990**, *9*, 301. However see: Gassman, P. G.; Deck, P. A.; Winter, C. H.; Dobbs, D. A.; Cao, D. H. *Organometallics* **1992**, *11*, 959.

(20) When this reaction is performed with in situ-generated **4**, excess Me_3SiCl (*ca.* 8 equiv) is used in order to account for reaction with intermediates **5** and **6**.

mL). The extract was filtered, concentrated to 50 mL, and cooled to −75 °C. After 4 d, red-orange crystals were collected by filtration and dried under vacuum (743 mg, 65.2%). Crystals suitable for X-ray analysis were obtained by crystallization (4 d) from hexanes. Anal. Calcd for $C_{24}H_{30}N_2SiZr$: C, 61.88; H, 6.49; N, 6.01. Found: C, 61.60; H, 6.31; N, 5.87. ^{1}H NMR (C_6D_6): δ 7.58 (d, J = 8 Hz, 2 H, indenyl), 7.51 (d, J = 8 Hz, 2 H, indenyl), 6.95 (pseudo t, J = 7 Hz, 2 H, indenyl), 6.86 (d, J = 3 Hz, 2 H, C_5 indenyl), 6.70 (pseudo t, J = 7 Hz, 2 H, indenyl), 6.21 (d, J = 3 Hz, 2 H, C_5 indenyl), 2.48 (s, 12 H, NMe_2), 0.79 (s, 6 H, $SiMe_2$). ^{13}C{^{1}H} NMR (toluene-d_8): δ 135.1 (C), 131.2 (C), 125.8 (CH), 124.1 (CH), 124.0 (CH), 122.9 (CH), 115.8 (CH), 109.9 (CH), 97.9 (C), 47.8 (NMe_2), −1.4 ($SiMe_2$).

***meso*-(SBI)Zr(NMe$_2$)$_2$ (*meso*-4)** was observed by ^{1}H NMR as a minor product (usually 5−10%) of the reaction of (SBI)H_2 and $Zr(NMe_2)_4$ under the above conditions. ^{1}H NMR (C_6D_6): the indenyl resonances are overlapped and obscured; δ 5.98 (d, J = 3 Hz, 2 H, C_5 indenyl), 2.99 (s, 6 H, NMe_2), 1.70 (s, 6 H, NMe_2), 1.04 (s, 3 H, $SiMe_2$), 0.51 (s, 3 H, $SiMe_2$).

***meso*-(μ-η^5:η^5-SBI){Zr(NMe$_2$)$_3$}$_2$ (*meso*-5).** A solution of (SBI)H_2 (0.547 g, 1.90 mmol) in toluene (100 mL) was added dropwise to a solution of $Zr(NMe_2)_4$ (1.12 g, 4.15 mmol) in toluene (100 mL) at 25 °C over 1 h. The pale orange solution was stirred for 21 h at 25 °C; the NMe_2H was allowed to escape from the reaction vessel via an oil bubbler . The solvent was removed under reduced pressure yielding an oily orange solid. ^{1}H NMR analysis of the oil showed that (μ-η^5:η^5-SBI){Zr(NMe$_2$)$_3$}$_2$ (**5**) was present in 85% yield in a *rac*/*meso* ratio of 1/2. The solid was extracted with hexanes (50 mL), and the extract was filtered, concentrated to 15 mL, and cooled to −80 °C for 7 d. Filtration afforded pure *meso*-(μ-η^5,η^5-SBI){Zr(NMe$_2$)$_3$}$_2$, as a pale orange crystalline solid, which was dried under vacuum (385 mg, 34.0%). Crystals suitable for X-ray analysis were obtained by crystallization (7 d) from hexanes. Anal. Calcd for $C_{32}H_{54}N_6SiZr_2$: C, 52.41; H, 7.42; N, 11.46. Found: C, 52.28; H, 7.34; N, 11.10. ^{1}H NMR (C_6D_6): δ 7.66 (d, J = 8 Hz, 2 H, indenyl), 7.61 (d, J = 8 Hz, 2 H, indenyl), 7.01 (pseudo t, J = 8 Hz, 2 H, indenyl), 6.94 (pseudo t, J = 8 Hz, 2 H, indenyl), 6.50 (d, J = 3 Hz, 2 H, C_5 indenyl), 6.40 (d, J = 3 Hz, 2 H, C_5 indenyl), 2.74 (s, 36 H, NMe_2), 0.90 (s, 3 H, $SiMe_2$), 0.85 (s, 3 H, $SiMe_2$). ^{13}C{^{1}H} NMR (C_6D_6): δ 132.1 (C), 130.1 (C), 125.9 (CH), 125.8 (CH), 123.0 (2 CH), 122.6 (CH), 105.6 (C), 102.6 (CH), 44.5 (NMe_2), 1.9 ($SiMe_2$), 0.6 ($SiMe_2$).

***rac*-(μ-η^5:η^5-SBI){Zr(NMe$_2$)$_3$}$_2$ (*rac*-5)** was observed as a minor product in the synthesis of *meso*-**5** and was characterized by ^{1}H NMR. ^{1}H NMR (C_6D_6): δ 7.51 (d, J = 8 Hz, 2 H, indenyl), 7.24 (d, J = 8 Hz, 2 H, indenyl), 6.81 (pseudo t, J = 8 Hz, 2 H, indenyl), 6.80 (d, J = 3 Hz, 2 H, C_5 indenyl), 6.66 (pseudo t, J = 8 Hz, 2 H, indenyl), 6.56 (d, J = 3 Hz, 2 H, C_5 indenyl), 2.77 (s, 36 H, NMe_2), 0.91 (s, 6 H, $SiMe_2$).

Characterization of (η^5-C$_9$H$_6$SiMe$_2$C$_9$H$_7$)Zr(NMe$_2$)$_3$ (6). A solution of $Zr(NMe_2)_4$ (**2**) (27 mg, 0.10 mmol) in C_6D_6 was added to a solution of *rac*-(SBI)H_2 (**3**) (26 mg, 0.090 mmol) at 25 °C, and the reaction was monitored by ^{1}H NMR. After 10 min, **2** was completely consumed and **6a,b** (82%), **6c** (4%), *rac*-**5** and *meso*-**5** (14%), unreacted **3,** and NMe_2H were present. Key ^{1}H NMR (C_6D_6) data for **6a**−**c** are listed below; the indenyl resonances are overlapped and obscured. **6a**: δ 6.20 (d, 1 H, J = 3 Hz, C_5 indenyl), 3.84 (s, 1 H, bridgehead), 2.73 (s, 18 H, NMe_2), 0.44 (s, 3 H, $SiMe_2$), −0.03 (s, 3 H, $SiMe_2$). **6b:** δ 3.82 (s, 1 H, bridgehead), 2.73 (s, 18 H, NMe_2), 0.56 (s, 3 H, $SiMe_2$), −0.04 (s, 3 H, $SiMe_2$). **6c:** δ 3.10 (s, 2 H, C_5), 2.76 (s, 18 H, NMe_2), 0.75 (s, 3 H, $SiMe_2$), 0.71 (s, 3 H, $SiMe_2$).

***rac*-(SBI)ZrCl$_2$ (*rac*-1). (a) NMR Scale.** An NMR tube was charged with *rac*-**4** (3.0 mg, 0.0064 mmol), Me_3SiCl (4.3 mg, 0.040 mmol), and C_6D_6 (0.5 mL). The tube was maintained at 23 °C and monitored periodically by ^{1}H NMR. After 30 min the solution was pale orange in color and the conversion to *rac*-(SBI)$ZrCl_2$ was 65% complete. After 5 h the solution was bright yellow and conversion to *rac*-(SBI)$ZrCl_2$ was complete; no *meso*-(SBI)$ZrCl_2$ was detected. ^{1}H NMR data are consistent with the literature data.[4] ^{1}H NMR (C_6D_6): δ 7.38 (d J = 8 Hz, 2 H, indenyl), 7.22 (d, J = 8 Hz, 2 H, indenyl), 7.15 (pseudo t, J = 7 Hz, 2 H, indenyl), 6.85 (pseudo t, J = 7 Hz, 2 H, indenyl), 6.80 (d, J = 3 Hz, 2 H, C_5 indenyl), 5.75 (d, J = 3 Hz, 2 H, C_5 indenyl), 0.54 (s, 6 H, $SiMe_2$).

(b) Preparative Scale. A three-neck round bottom flask was charged with (SBI)H_2 (5.40 g, 18.7 mmol), $Zr(NMe_2)_4$ (5.00 g, 18.7 mmol), hexamethylbenzene (0.25 equiv, internal standard), and hexane (325 mL). The flask was fitted with a water-cooled fractional distillation column (25 cm × 20 mm) packed with 3 mm glass helices. The mixture was refluxed for 21 h with an N_2 flow over the top of the column and then cooled to 25 °C. The volatiles were removed under reduced pressure, benzene (200 mL) and Me_3SiCl (17.5 mL, 138 mmol) were added, and the mixture was stirred for 24 h. The mixture was filtered and the solid was dried under reduced pressure, affording *rac*-(SBI)$ZrCl_2$ (4.52 g, 53.9% from $Zr(NMe_2)_4$) as a yellow solid.

***rac*-(SBI)ZrMe$_2$ (rac-7). (a) NMR Scale.** An NMR tube was charged with *rac*-(SBI)$Zr(NMe_2)_2$ (20 mg, 0.043 mmol), Al_2Me_6 (19 mg, 0.13 mmol), and C_6D_6 (0.5 mL). The tube was maintained at 23 °C and monitored periodically by ^{1}H NMR. After 30 min the solution was bright yellow and conversion to *rac*-(SBI)$ZrMe_2$ was complete with no sign of isomerization. ^{1}H NMR (C_6D_6): δ 7.45 (d J = 8 Hz, 2 H, indenyl), 7.20 (d, J = 8 Hz, 2 H, indenyl), 7.13 (pseudo t, J = 7 Hz, 2 H, indenyl), 6.82 (pseudo t, J = 7 Hz, 2 H, indenyl), 6.69 (d, J = 3 Hz, 2 H, C_5 indenyl), 5.67 (d, J = 3 Hz, 2 H, C_5 indenyl), 0.53 (s, 6 H, $SiMe_2$), −0.99 (s, 6 H, $ZrMe_2$).

(b) Preparative Scale. A solution of $AlMe_3$ (2.20 g, 30.6 mmol) in hexanes (100 mL) was added dropwise to an orange solution of *rac*-(SBI)$Zr(NMe_2)_2$ (2.51 g, 5.37 mmol) in toluene (150 mL) at 0 °C over 2 h. The yellow solution was stirred for 2 h at 23 °C. The solvent was removed under reduced pressure yielding a yellow solid, which was washed with pentane (20 mL) to remove the aluminum coproducts. The solid was dried under vacuum for 24 h, affording pure *rac*-(SBI)$ZrMe_2$ (1.99 g, 92%). The ^{1}H NMR data are consistent with literature data.[21]

Acknowledgment. This research was supported by the National Science Foundation (Grant CHE-9413022; R.F.J.). The authors wish to acknowledge Dr. Il Kim for the initial in situ methylation of *rac*-**4**.

Supporting Information Available: Text describing X-ray procedures, tables of X-ray data, atom positional and thermal parameters, and bond distances and angles, and ORTEP diagrams (16 pages). Ordering information is given on any current masthead page.

OM960104B

(21) Bochmann, M.; Lancaster, S. J.; Hursthouse, M. B.; Abdul Malik, K. M. *Organometallics* **1994**, *13*, 2235.